Heterogeneous responses to embryonic critical period perturbations within the *Drosophila* larval locomotor circuit.

Niklas Krick*[1], Jacob Davies*[2], Bramwell Coulson*[2], Daniel Sobrido-Cameán[1], Michael Miller[1], Matthew C. W. Oswald[1], Aref A. Zarin[3], Richard Baines[#2], Matthias Landgraf[#1]

* = joint first authors

= joint senior and corresponding authors

Affiliations:

1 Department of Zoology, University of Cambridge, Cambridge CB2 3EJ, United Kingdom

2 Division of Neuroscience, School of Biological Sciences, Faculty of Biology, Medicine and Health, Manchester Academic Health Science Centre, University of Manchester, Manchester M13 9PL, United Kingdom

3 Department of Biology, Texas A&M University, College Station, Texas 77843-3258

Abstract

As developing neural circuits become functional, they undergo a phase of heightened plasticity that facilitates network tuning in response to intrinsic and/or extrinsic stimuli. These developmental windows are termed critical periods (CPs), because perturbations during, but not outside the CP, can lead to lasting and significant changes, such as the formation of sub-optimal or unstable networks. How separate, but connected elements, within a network might respond differently to a CP perturbation is not well understood. To study this, we used the locomotor network of the *Drosophila* larva as an experimental model, using heat stress as an ecologically relevant CP stimulus. We show that increasing ambient temperature elevates locomotor network activity. When applied during the embryonic CP, heat stress leads to the formation of a network that has suboptimal output; causing larvae to crawl more slowly and requiring longer to recover from electroshock-induced seizures, indicative of decreased network stability. Within the central nervous system, we find transient embryonic CP perturbation leads to increased synaptic drive from premotor interneurons to motoneurons, which in turn adopt reduced excitability. In contrast, the peripheral

neuromuscular junction, maintains normal synaptic transmission, despite significant structural changes of synaptic terminal overgrowth and altered postsynaptic receptor field composition. Overall, our data demonstrate that connected elements within a network respond differentially to a CP perturbation. Our results suggest a sequence, or hierarchy, of network adjustment during developmental CPs, and present the larval locomotor network as a highly tractable experimental model system with which to study CP biology.

Introduction

During nervous system development, critical periods (CPs) are transient windows of heightened plasticity, which are fundamental to the emergence of appropriate network function. As a consequence, networks are particularly vulnerable to activity perturbations during a CP, which can result in lasting structural and/or functional changes, while comparable perturbations outside the CP are less impactful (Coulson et al., 2022; Reh et al., 2020). The functions and concepts of CPs have traditionally been investigated in the visual system of mammals (Hensch, 2005; Hensch and Quinlan, 2018; Hubel and Wiesel, 1970) and imprinting of birds (Hess, 1975; Horn, 2004). More recently, CPs have also been identified and investigated across a range of species and neuronal ensembles, from networks underlying the development of speech (Harrison et al., 2005) to motor behaviour of rats (Soiza-Reilly and Azcurra, 2009), fish (Hageter et al., 2023) and insects (Dombrovski and Condron, 2021; Giachello and Baines, 2015). The presence of a CP in developing networks is therefore increasingly considered a universal phenomenon. The precise changes within networks and associated mechanisms, as they occur during normal development, as well as those resulting from perturbations during a CP, are not well understood. This is in part due to the complexity of many of the experimental model systems, notably mammalian cortical systems that have been the predominant model for studying CPs.

To overcome this technical obstacle, we have utilized the comparatively simpler nervous system of the fruit fly larva, *Drosophila melanogaster*, with which to study CPs. Though an insect, *Drosophila* displays CPs with features that suggest commonalities to mammalian CPs (for review see: Coulson et al., 2022). Currently, the best characterised CP during *Drosophila* development is one that occurs during embryogenesis, linked to the emergence of normal locomotor network output (Carreira-Rosario et al., 2021; Corke et al., 2025;

Coulson et al., 2022; Crisp et al., 2008, 2011; Ackerman et al., 2021; Fushiki et al., 2013; Giachello et al., 2021; Giachello and Baines, 2015; Hunter et al., 2024; Williamson et al., 2021; Zeng et al., 2021). This experimental system benefits from the comprehensively annotated connectome of the *Drosophila* larval nervous system (Giachello et al., 2020; Heckman and Doe, 2022; Valdes-Aleman et al., 2021; Winding et al., 2023) as well as an unparalleled set of genetic tools for manipulating identified neurons with both spatial and temporal precision (Simpson, 2009). Combined with imaging and electrophysiological techniques, this model system enables investigation of cellular responses to CP manipulations at the level of identified cells and synapses (Carreira-Rosario et al., 2021; Coulson et al., 2022; Crisp et al., 2008, 2011; Fushiki et al., 2013; Giachello et al., 2021; Giachello and Baines, 2015; Hunter et al., 2024; Williamson et al., 2021; Zeng et al., 2021).

Neuronal activity manipulations during the CP of *Drosophila* embryos have been shown to cause decreased network stability. This manifests in significantly longer times required for larvae to recover from a strong activity challenge, such as electric shock-induced seizures (Coulson et al., 2022; Giachello et al., 2021; Giachello and Baines, 2015; Hunter et al., 2024, 2021). The premise that balanced network activity during the CP is necessary for stable, resilient networks to form has been explicitly supported by findings from our recent studies (Giachello et al., 2021; Giachello and Baines, 2015; Hunter et al., 2024). By extension, rectifying activity manipulations during identified CPs could have therapeutic potential (Nardou et al., 2023).

While experimental perturbations of neuronal activity during development have been a useful methodological approach for studying CPs as a phenomenon and the associated biological mechanisms, such manipulations might seem artificial in the context of normal development. Most animals are not warm-blooded and in poikilothermic animals, such as *Drosophila,* changes in ambient temperature, daily as well as seasonal, lead to changes in behavioural activity, likely caused by changes in neuronal and network activity (Lee and Montell, 2013; Powsner, 1935). Studies from the crustacean stomatogastric nervous system showed that these minimal networks produce a characteristic, rhythmic firing pattern, which is robustly maintained across a range of external temperatures. Importantly, neuronal network properties were adapted relative to the long-term temperatures that crabs had experienced, resulting in significantly different upper “crash temperatures” at which networks ceased to function (Marder, 2023; Marder and Rue, 2021). In *Drosophila,* the temperature experienced by late embryos determines larval locomotor output, including crawling speed and social feeding behaviour (Williamson et al., 2021). Similarly, studies on the *Drosophila*

adult visual and olfactory systems showed that neuronal wiring properties and associated behaviours of adults are determined by the temperature experienced during a second CP of *Drosophila,* which takes place during pupariation (Chodankar et al., 2020; Kiral et al., 2021; Züfle et al., 2025), a phase of extensive network remodelling (Baumann et al., 2024; Leier et al., 2025; Lowe et al., 2023; Nelson et al., 2024).

In this study, we investigated ambient temperature as an ecologically relevant stimulus. To gain insights at the level of single, identified connected cells, we focused on the neuromuscular system of the *Drosophila* larva, and discovered that the components of this network respond differently to transient heat stress, when experienced during the CP. Specifically, we find that elevated temperature increases neuronal activity, and that transient heat stress during the locomotor CP causes long term reduced network stability, similar to the effects of neuronal activity manipulations (Giachello et al., 2021; Giachello and Baines, 2015; Hunter et al., 2024). These changes are accompanied by presynaptic terminal overgrowth at the neuromuscular junction (NMJ) and changes in postsynaptic neurotransmitter receptor composition, though synaptic transmission is homeostatically regulated and remains normal. In contrast, within central circuitry, we find that transient heat stress leads to reduced excitability of motoneurons, potentially as a response to enhanced synaptic drive from premotor interneurons. Overall, this study presents a first comprehensive analysis of how several interconnected elements of a defined locomotor network develop in response to CP perturbation by heat stress, an ecologically relevant stimulus.

Results

Temperature manipulation during the locomotor CP leads to an unstable crawling network.

We had previously identified a CP of nervous system development in late embryogenesis, from 17 – 19 hrs after egg laying (AEL), equivalent to 80-90% of embryonic development (Giachello and Baines, 2015). Perturbation of network activity during this developmental time window, pharmacologically or optogenetically, leads to the formation of an unstable, seizure prone network. These phenotypes manifest most clearly upon acute activity challenges. For example, an electric shock administered to late larvae, that during their embryonic CP had experienced an activity manipulation, causes seizures with recovery times that are significantly longer compared to unmanipulated controls. Because large-scale

activity manipulations during the embryonic CP are artificial, We asked to what extent changes in environmental conditions, that embryos might normally encounter, might also alter network development. As poikilothermic animals, *Drosophila* development strongly depends on ambient temperature (Powsner, 1935). Several studies have shown that temperature experiences during development alter neuronal wiring as well as behaviours in larval and adult flies (Kiral et al., 2021; Williamson et al., 2021; Züfle et al., 2025).

We tested heat stress of 32ºC (Scialò et al., 2015), which is known to be experienced by *Drosophila melanogaster* (Williamson et al., 2021), i.e. 7ºC above the evolved temperature preference of 25ºC (Ashburner et al., 1983). We exposed embryos to 32ºC heat stress before, during, or after the embryonic CP, then returned the embryos to the preferred temperature of 25ºC. After four days, at the end of larval development, we measured the speed of recovery from electric shock-induced seizures, as a proxy for network stability. Transient heat stress experienced before or after the embryonic CP did not result in a change from unmanipulated controls (i.e. no change in seizure response), while in animals that had experienced 32ºC heat stress during the embryonic CP (i.e. between 17 – 19 hrs) had significantly prolonged recovery times from induced seizure, indicative of reduced network stability (Fig. 1A). Several studies had previously shown that increasing temperature leads to increased activity in the locomotor network (Oswald et al., 2018; Sigrist et al., 2003; Zhong and Wu, 2004). We tested this directly by functional imaging in isolated CNS, measuring spontaneous calcium transients from motoneurons. Specifically, we expressed GCaMP8f selectively in aCC motoneurons using *R94G06-GAL4*. Stepwise increases in temperature led to both, an increase in the GCaMP signal amplitude and in the frequency of rhythmic bursts. In contrast, CNSs kept at the control temperature of 25°C for the duration of functional imaging tended to show a decreasing GCaMP signal amplitude (Fig. 1B). These experiments suggest that increases in ambient temperature, above 25ºC, lead to concomitant increases in locomotor network activity. When those that occur during the embryonic CP, result in altered developmental outcomes, notably of sub-optimal, less stable networks.

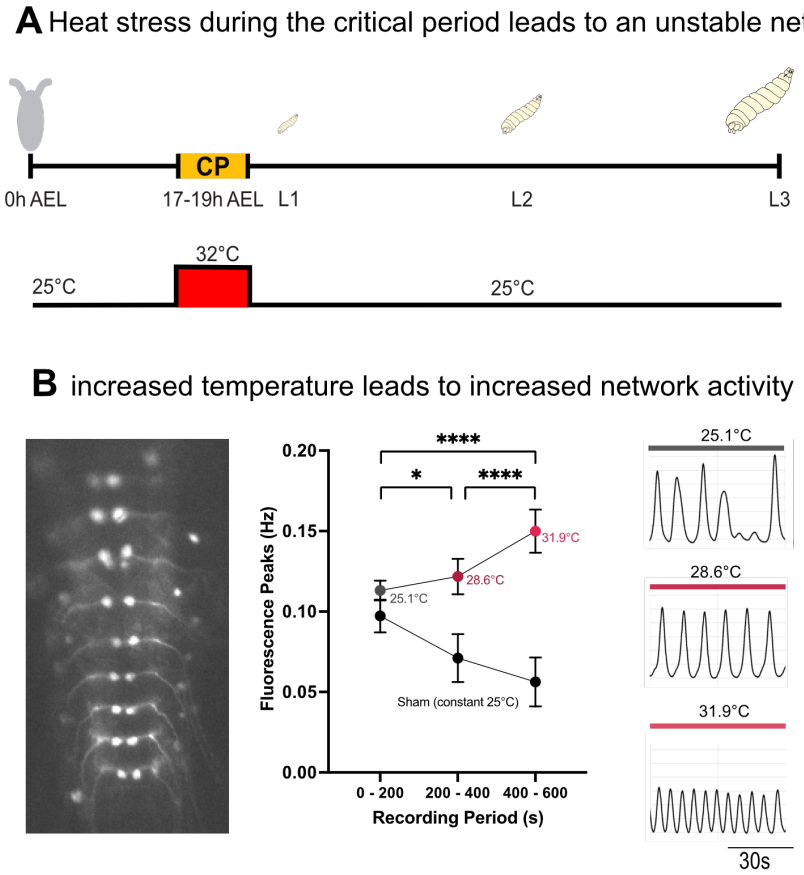

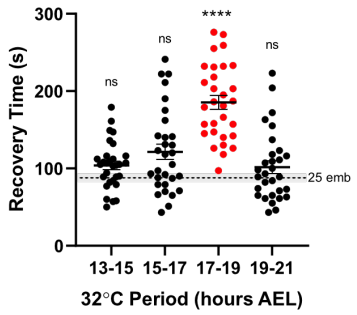

Figure 1: Transient heat stress during the critical period leads to unstable networks.

A Schematic representation of embryonic and larval development and temperature manipulation during embryogenesis. Embryos were kept at 32°C for 2 h either before (13-15 h, 15-17 h AEL), during (17-19 h AEL) or after (19-21 h AEL) the locomotor network CP. **B** Acute increase of temperature leads to increased network activity, as measured with the fluorescent calcium indicator GCaMP8f expressed in segmentally repeated aCC motoneurons in isolated central nervous systems; while constant 25°C leads to reduced activity over time.

Temperature manipulation during the embryonic CP leads to changes in larval NMJ morphology and composition.

To investigate structural and functional changes that result from a CP heat stress perturbation we first focused on the well characterised, and easy to access, peripheral neuromuscular junction (NMJ). Specifically, we focused on the NMJ of dorsal acute muscle 1 (DA1), which is innervated by the aCC motoneuron, a cell that has been the focus of our previous studies centred around CP perturbations (Fig. 2A) (Baines et al., 2001, 1999; Fujioka et al., 2003; Hunter et al., 2024; Landgraf et al., 2003; Giachello et al., 2021; Giachello and Baines, 2015). Because temperature manipulations outside the CP did not lead to an unstable network (Fig. 1A), we adopted a simplified experimental paradigm of putting embryos from a 6h egg collection to 32°C for 24h. This produces identical outcomes to heat stress limited to the CP, and it ensures that all embryos go through their CP during heat stress irrespective of minor variations in developmental timing or due to retention of

fertilised eggs. We find that embryonic heat stress leads to a significant overgrowth of the aCC motoneuron terminal (type Ib boutons) by the late larval stage, resulting in an increase in the number of boutons and active zones, while overall active zone density is not altered (Fig. 2B). On the postsynaptic side, embryonic CP heat stress causes an altered receptor composition: a selective reduction of the larger conductance GluRIIA subunit. Across the aCC NMJ, this leads to a reduced ratio of the larger conductance GluRIIA *versus* the lower conductance GluRIIB subunit (Fig. 2C-Cii).

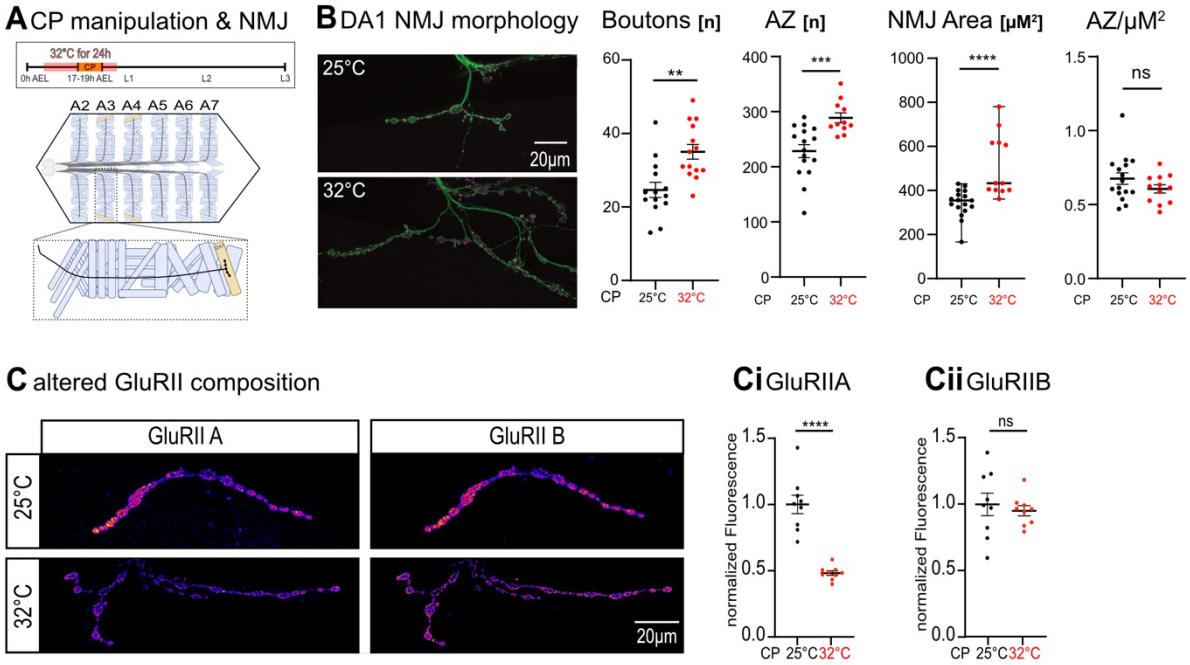

Figure 2: Morphological changes at the neuromuscular junction after critical period perturbation. A) Schematic of temperature manipulation during embryogenesis and location of dorsal acute muscle 1 (DA1) within a fillet dissected larva. Embryos collected over a 6h period were incubated at 32°C for 24h to guarantee heat stress exposure during the embryonic CP, 17-19 hours after egg laying. **B)** This results in a change of subsequent NMJ development with significant overgrowth of aCC presynaptic terminals (green) and an increase in bouton number and NMJ area. A concomitant increase in active zone number (magenta) results in a normal active zone density. **C)** Postsynaptically, CP heat stress result in a decrease of GluRIIA **(Ci)** while GluRIIB levels remain unaffected **(Cii).**

Despite morphological changes, larval NMJ physiology is not altered.

In view of the prominent changes in NMJ growth, morphology and postsynaptic glutamate receptor composition that result from heat stress (32°C) during the embryonic CP, we next assessed synaptic physiology at this NMJ. We used the two-electrode voltage clamp (TEVC) technique, initially measuring single pulse transmission across a gradient of external calcium concentrations. Despite the marked structural changes in manipulated animals, single pulse transmission was not significantly different between embryonically manipulated (32°C experience during their CP) and controls that experienced 25°C throughout (Fig. 3 A&B). Quantification of the number of release sites utilised per action potential and quantal size (Jusyte et al., 2023) also showed no statistically significant difference between CP-manipulated and control specimens (Fig. 3C). Next, we quantified the size of the readily releasable pool of synaptic vesicles by recording responses to a high frequency train of action potentials (Fig. 3D), then plotting the cumulative amplitude of responses to the first 60 pulses and linearly back extrapolating through the last 20 pulses to y=0 (Fig. 3E). This also did not show a significant difference between CP-manipulated and control animals (Fig. 3F). Though we noticed that during the 60Hz pulse train, NMJs in CP-manipulated specimens exhibited an increased facilitation during the first 10 pulses, indicating a slight reduction in release probability of the presynaptic terminal (Fig. 3D). Last, we tested if the NMJ remained able to adjust homeostatically to acute changes in synaptic transmission. We utilized the well-established method of acutely blocking glutamate receptors with Philanthotoxin (PhTx), a GluRIIA blocker, to induce presynaptic homeostatic potentiation (Frank et al., 2006; Genç and Davis, 2019; Müller and Davis, 2012). Acute GluRIIA blockade by a 10 min incubation with PhTx caused a significant reduction mEPSC amplitude while evoked EPSC amplitude remained unchanged in both controls and CP-manipulated specimens. Calculating quantal content shows that in response to acute GluRIIA blockade, both control and CP-manipulated animals are indeed able to induce presynaptic homeostatic potentiation by increasing quantal content (Fig. 3G-Giii). While establishing baseline conditions, we found mEPSC amplitudes and quantal content to be comparable between controls and CP-manipulated animals Fig. 3G-Giii). This was contrary to expectation in light of the overall reduction in the GluRIIA/B ratio that results from a CP heat stress manipulation. However, we noticed that reductions in GluRIIA signal were most pronounced in proximal regions of the NMJ; while distal boutons, which have a higher probability of release under low frequency stimulation regimes (Peled and Isacoff, 2011), have normal levels of GluRIIA. The preferred recruitment of distal boutons for release could explain the apparent lack of effect on mEPSC amplitude. Overall, we conclude that despite the significant structural

changes that emerge by late larval stage following a transient embryonic 32°C heat stress experience, synaptic physiology at the late larval NMJ remains normal. Moreover, when considering the unstable network phenotype, as manifest by increased recovery times from electric shock-induced seizures, our finding that synaptic transmission at the NMJ remained normal suggests that network instability likely originates from changes within the central locomotor circuitry.

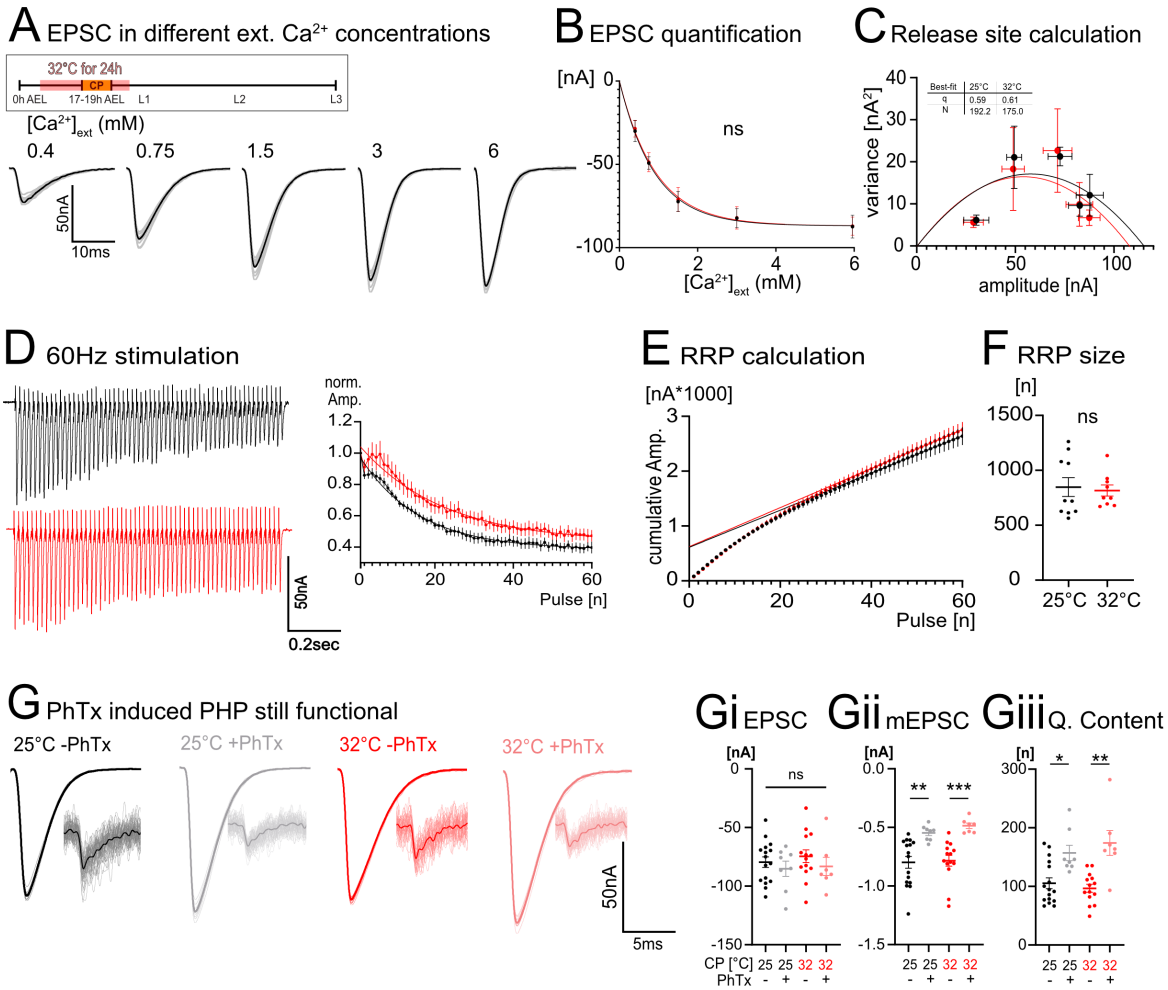

Figure 3: Physiological NMJ properties after 32°C perturbation. A) Representative traces of control two electrode voltage clamp recordings across a gradient of external calcium concentrations. **B)** Postsynaptic current amplitude is not altered between control and CP-manipulated animals at any given external calcium concentration. **C)** Plotting postsynaptic current amplitude against its variety to calculate quantal size (q) and the number of release sites being used (N), also did not show a significant difference between control and CP-manipulated animals. To measure readily releasable pool size, a 60Hz stimulus train was applied for 1s **(D)** where we could observe a slight increase in facilitation over the first 10 pulses in specimens that in their embryonic stage had experienced heat stress of 32°C. Cumulative amplitude was plotted over time and a linear regression was back extrapolated through the last 20 pulses **(E)**. The y intercept was divided by the Mini size of the same trace to calculate the readily releasable pool size. **G-Giii)** NMJs in CP-manipulated specimens have normal EPSC and mEPSC amplitudes and quantal content. Acute application of the GluRIIA blocker PhTx reliably induced presynaptic homeostatic potentiation in controls and 32°C CP-manipulated animals.

Motoneurons display reduced excitability and receive increased synaptic input following CP perturbation by heat stress.

We noted that in CP-manipulated larvae, motor axons required increased stimulation voltage to reliably induce action potentials. This hints at motoneurons in CP-manipulated larvae having acquired reduced excitability. To directly test motoneuron excitability, we used whole cell patch clamp to measure evoked action potential firing, as a measure of excitability of the aCC motoneuron. These measures were made in the presence of mecamylamine (200 μM in external saline) to block endogenous cholinergic excitatory synaptic drive. Action potential firing of aCC was evoked using injection of current steps (4pA). We found that in late L3, aCC had significantly decreased excitability following an embryonic CP experience of 32°C heat stress (Fig. 4A). These results are comparable to, and validate, results obtained after optogenetic locomotor network activity manipulation during the same embryonic CP (Giachello and Baines, 2015). In previous studies, we had shown with recordings from aCC that its synaptic drive is enhanced following transient CP manipulations of network activity, using optogenetic or pharmacological means to induce network over-excitation, or genetic overactivation of neurons, as in *para*^{bss} seizure mutants (Giachello and Baines, 2015; Hunter et al., 2024). Specifically, endogenous excitatory cholinergic synaptic currents, termed spontaneous rhythmic currents (SRCs), were increased in duration, though not in amplitude, following network activity manipulations during the CP (Giachello et al., 2019; Giachello and Baines, 2015). We asked if heat stress during the CP led to similar changes. Indeed, in late larvae that had transiently experienced heat stress during their embryonic CP, SRCs recorded from aCC motoneurons were significantly increased in duration, though with amplitude unchanged (Fig. 4Bi). Note these SRC recordings were undertaken in the absence of mecamylamine and suggest an increase in premotor network activity. Together with the decrease in membrane excitability of aCC, these observations are compatible with the idea that motoneurons might have undergone homeostatic adjustment in response to an increase in premotor excitatory synaptic drive caused by the CP manipulation.

To test that hypothesis, we recorded synaptic drive to aCC, under whole cell patch clamp configuration, while optogenetically activating a specific and strongly connected excitatory premotor interneuron, termed “A27h” (Hunter et al., 2023). Because motoneurons are quiescent without synaptic drive, a small amount of current was injected to aCC to maintain a modest and consistent mean firing frequency of ~10-20 Hz. As might be expected, and as per our previous study (Hunter et al., 2024), acute optogenetic activation of the A27h premotor excitor resulted in increased aCC firing frequency. Significantly, this increase was

greater in larvae that had been exposed to heat stress during their embryonic CP, compared to controls (Fig 4.Bii). This observation supports the hypothesis that heat stress during the embryonic CP results in increased excitatory drive from central interneurons, which is then countered by postsynaptic motoneurons through reduction in their excitability.

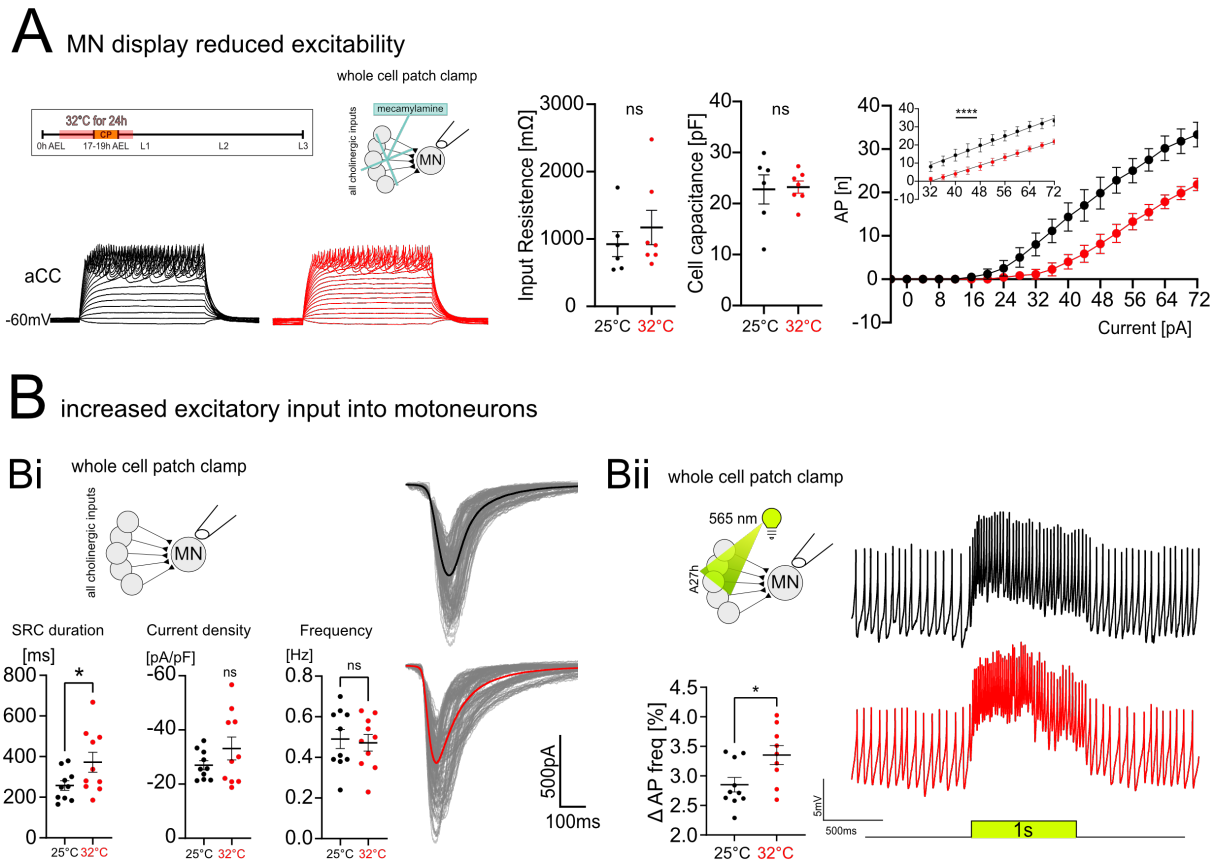

Figure 4: Larval motoneurons display reduced excitability and increased synaptic input after an embryonic 32°C CP-manipulation. A aCC motoneurons at the late third instar larval stage, isolated from excitatory synaptic input. Motoneurons in specimens, which during the embryonic CP had transiently experienced 32°C heat stress, show significant reduction in excitability relative to controls. **B** Left: whole cell patch clamp recordings from the aCC motoneuron reveal an increase in spontaneous rhythmic current duration several days after embryos had experienced transient 32°C heat stress during the CP. Right: targeted optogenetic activation (using Chronos) of a premotor excitatory interneuron (A27h) showed that A27h input is increased in late larvae that as embryos had experienced 32°C heat stress during the CP.

Homeostatic adjustments of the aCC motoneuron result in normal endogenous firing patterns.

If the adjustments displayed by the aCC motoneuron are indeed a homeostatic response, then one might predict this to be a mechanism to maintain the endogenous level of motoneuron activity. To test this, we used whole cell patch recordings from aCC motoneurons, in isolated nerve cords of late third instar larvae. As hypothesized, our

recordings show no significant differences in endogenous motoneuron activity as a result of embryonic CP heat stress, measured by burst rate, burst duration, or action potentials per burst (Fig. 5A). Finally, to test if homeostatic adjustments of motoneurons translate to normal muscle output, we recorded spontaneous synaptic drive from muscles in a semi-intact preparation with an intact nervous system attached. Current clamp recordings from the DA1 muscle, while supressing muscle contractions using nifedipine (50µM) (Dyson et al., 2022; Kratschmer et al., 2021), showed no significant differences in spontaneous burst frequency or duration, nor the overall time spent bursting (Fig. 5B), between controls and CP heat stress-manipulated specimens. Therefore, we conclude that CP manipulations act primarily on the cells of the premotor circuitry, namely excitatory premotor interneurons as tested in this study. Changes in the motoneurons can be seen to constitute secondary homeostatic adjustments in response to those premotor network changes.

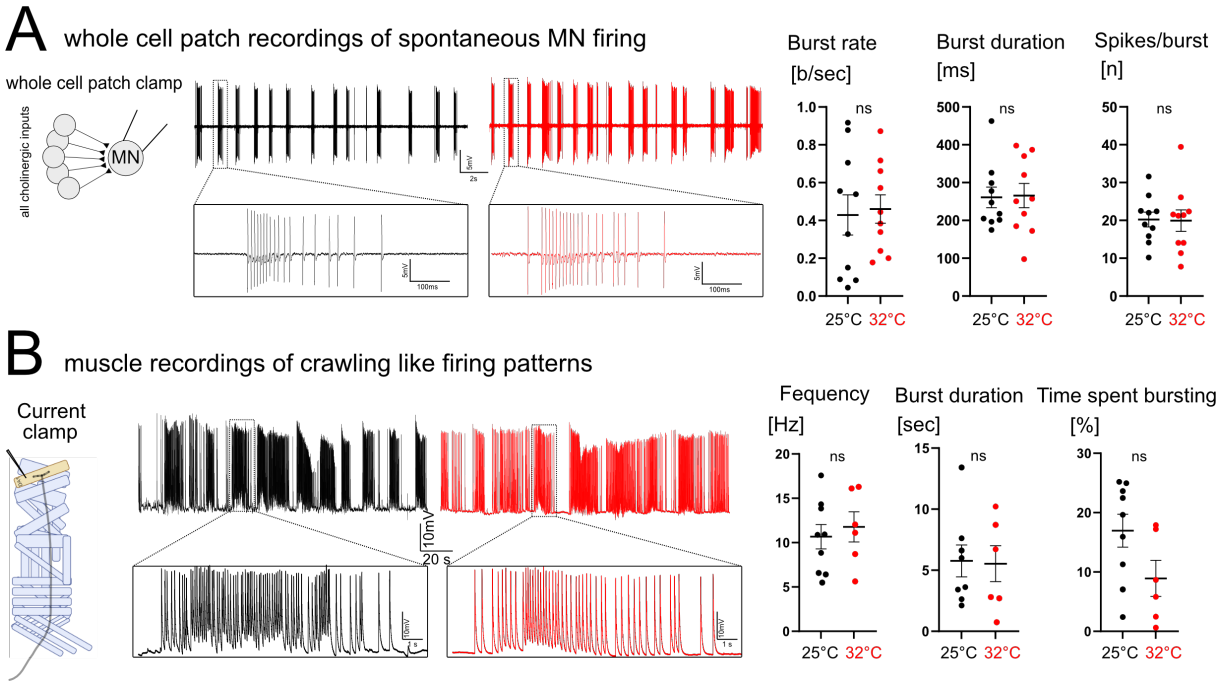

Figure 5: Spontaneous larval motoneuron and muscle firing properties and are unchanged after embryonic temperature challenge. A Monitoring spontaneous firing by loose cell patch clamp recordings from the aCC motoneuron in a late third instar larval nerve cord did not show a significant difference between CP-manipulated specimens and controls. **B** Measuring muscle output of motoneuron spontaneous firing by current clamp recordings from the DA1 muscle in late third instar larvae showed that animals are able to produce normal motoneuron firing output to the muscle, irrespective of embryonic experience.

Inter-segment wave propagation speed is reduced following embryonic critical period perturbation.

To test how excitatory premotor interneurons are affected following a transient embryonic 32°C CP manipulation, we expressed the calcium indicator GCaMP8f in A27h interneurons, and in isolated 3rd instar nerve cords recorded the propagation of neuronal activation waves across abdominal segments, indicative of fictive locomotion (Fig.6A) (Streit et al., 2016; Pulver et al., 2015). These experiments show that a transient 32°C exposure during the embryonic CP leads to a significant increase in the time required for this neuronal activity wave propagation, as compared to controls. This mirrors a decrease in crawling speed in intact larvae (Fig.6B). Because our electrophysiological analyses showed that motoneuron firing patterns and output to the muscle remain normal after a 32°C CP manipulation (Fig.3-5), these results further support the hypothesis that it is the lasting changes to the central premotor circuitry, rather than to the motoneurons, which are responsible for the changes in crawling behaviour, and likely also for network instability.

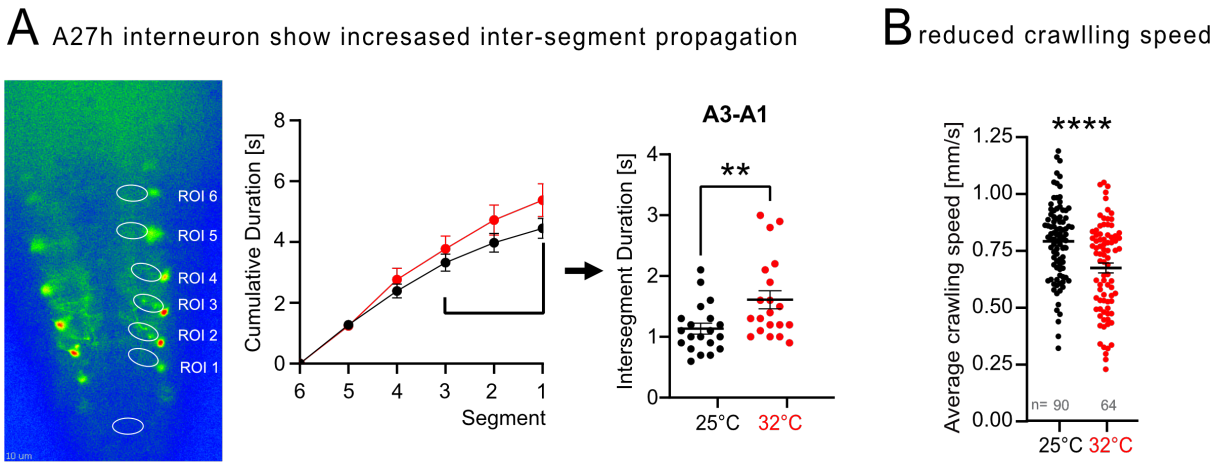

Figure 6: CP manipulation causes reduced speed of activity wave propagation and larval crawling. A Functional imaging of A27h premotor interneurons using GCaMP8f in isolated CNSs from late larvae that previously had experienced transient 32°C heat stress during their embryonic CP. Propagation of the activity wave is slowed down, due to an increase in intersegment duration, notably between anterior segments, e.g. A3 and A1. **B** In intact animals, network activity is similarly altered: CP heat stress (32°C) leads to a significant reduction in larval crawling speed, as compared to controls (25°C).

Discussion

An experimental model system with which to study CP biology

In this study we have utilised the larval neuromuscular system as an experimental model with which to study the role of CP-regulated plasticity across interconnected cells within a defined circuit. We have identified 32ºC heat stress as an ecologically relevant CP stimulus: transient exposure of embryos to 32ºC during the previously defined CP for the developing CNS (17-19 hours after egg laying) leads to lasting changes in subsequent nervous system development, resulting in reduced network stability which is reflected by an increased susceptibility to electro-shock induced seizures. As is characteristic for CPs, the same manipulation before or after this defined developmental window has no lasting effect on nervous system properties or animal behaviour. Calcium imaging of motoneurons showed that stepwise increases in ambient temperature cause acute increases of rhythmic locomotor network activity. This is in line with past studies, which had demonstrated the well-established link between temperature and neuronal activity in this same experimental system (Zhong and Wu, 2004). It is perhaps, therefore, not surprising that 32ºC heat stress during the embryonic CP of nervous system development causes outcomes that are comparable to neuronal activity manipulations (pharmacological or genetic) during this developmental window (Giachello et al., 2021; Giachello and Baines, 2015; Hunter et al., 2024).

Different cell types respond differently to CP manipulations.

A particular strength of the *Drosophila* larval motor system is the accessibility of interconnected network elements. We focused on a small part of the locomotor network: an excitatory premotor interneuron (A27h) connected to a motoneuron (aCC), and its postsynaptic target body wall muscle (DA1). Following transient application of heat stress as an ecologically relevant during the embryonic CP, we could identify that within this section of the locomotor network each of these three connected nodes responded differently. We observed increased excitatory drive from A27h interneurons to aCC motoneurons, while those motoneurons displayed homeostatic adaptation; namely, a decrease in excitability, leading to maintenance of normal firing patterns. At the presynaptic NMJ terminal in the periphery, in contrast, we documented normal synaptic transmission properties, despite a significant presynaptic terminal overgrowth. The latter might be a secondary adjustment to

a decrease in transmitter sensitivity by the muscle, which showed reduced GluRIIA levels along parts of the NMJ terminal.

The first observation to make is that the responses have been reproducible. This suggests that there might be direct cause-effect relationships at the cellular level, which can now be investigated in detail. An alternative interpretation is that activity patterns in this part of the network might be robustly canalised to affect reproducible outcomes. Second, the changes in neuronal excitability and synaptic transmission are compatible with a temporal sequence, or a functional hierarchy, during network maturation. For example, following an embryonic heat stress, premotor interneurons, potentially part of the central pattern generator (Carreira-Rosario et al., 2021; Zeng et al., 2021), increase their collective synaptic drive to postsynaptic motoneurons, which in turn reduce their excitability (Figure 4). Thus, the changes in motoneuron properties that we have characterised, we interpret as homeostatic responses to the increase in presynaptic excitatory drive from premotor interneurons. This implies a hierarchy, whereby the specification of premotor interneuron properties dominates that of their downstream integrators, the motoneurons. A sequence of cell type-specific maturation windows has recently been shown in the developing mouse neocortex. There, the somatostatin-expressing inhibitory interneurons differentiate early and promote spontaneous activity through inhibition of the later differentiating parvalbumin-expressing inhibitory interneurons (Mòdol et al., 2024).

NMJ structural development is affected by CP manipulations but not synaptic transmission.

Despite embryonic heat stress leading to significant NMJ structural changes, in terms of presynaptic terminal overgrowth (an average increase of active zone number by 30%) and overall reduction by 50% of GluRIIA, evoked transmission resulting from the firing of single action potentials in the motor axon remained normal. Closer inspection suggested that GluRIIA distribution was no longer homogenous in late larval NMJs if the animal had experienced heat stress during its embryonic CP. While GluRIIA levels were reduced proximally (axon entry point), distal boutons, in contrast, retained normal GluRIIA levels. Distal boutons had previously been shown to house release sites that are preferentially recruited under low frequency stimulation regimes (Peled and Isacoff, 2011). This could explain why we observed normal evoked transmission despite the significant reduction of GluRIIA at proximal sites. If this was the case, then one might expect high frequency

stimulation regimes, e.g. of 60 Hz, to recruit many other presynaptic sites for vesicle fusion, including the proximal sites that are apposed to postsynaptic densities with reduced GluRIIA. Although we did not conduct functional imaging to investigate this directly, a 60 Hz stimulation regime did indeed reveal increased facilitation in animals that experienced heat stress during their embryonic CP, indicating a reduction in presynaptic release probability across the whole NMJ. Though statistically not reaching significance, changes in release probability would be compatible with the idea that at sub-60 Hz stimulation a much larger fraction of synaptic release sites are recruited, including proximal sites with reduced GluRIIA (Figure 3D). That evoked synaptic transmission at the NMJ is not significantly affected by CP manipulations, is perhaps to be expected. A well-established feature of this synapse is that its transmission is tightly regulated to maintain consistency. The various NMJ plasticity mechanisms include presynaptic homeostatic potentiation (PHP), which we have shown to function effectively even after CP heat stress manipulation (Delvendahl and Müller, 2019; Frank et al., 2020, 2006; Goel and Dickman, 2021).

It is unlikely that structural changes at the NMJ contribute to making the nervous system less stable, or that they effect CP-regulated changes to larval behaviour, such as crawling speed or social feeding (Williamson et al., 2021). Based on previous CP manipulations targeted to various neuronal subsets (Giachello et al., 2021), it seems more likely that behavioural phenotypes, including reduced crawling speed and increased recovery times from electric shock-induced seizures, would be the consequence of changes in the central circuitry. Indeed, functional imaging of the excitatory premotor interneuron, A27h, showed that embryonic heat stress leads to networks with significantly slower intersegmental propagation of fictive locomotor waves, compatible with the reduced crawling speed seen in intact larvae (Figure 6). This contrasts with acute heat stress causing an increase in such fictive locomotor waves of activity (Figure 1B). Heat stress during the CP could cause a malfunctioning of pacemaker activity. Alternatively, the observed slowing of the CPG in larval stages could be a network-wide homeostatic response to an abnormally fast rate experienced due to heat stress exposure during the embryonic CP. We propose that the NMJ, because it is a large, readily accessible peripheral synapse whose development is altered following transient CP heat stress, could be serve as an experimental model for studying CP-associated mechanisms.

Acknowledgements

This work was made possible through support by a Walter Benjamin Programme Fellowship to NK by the Deutsche Forschungsgemeinschaft (DFG) KR5597/1-1, and funding from the Biotechnology and Biological Sciences Research Council (BBSRC) to ML (BB/V014943/1) and the Wellcome Trust, through a Joint Wellcome Trust Investigator Award to RAB and ML (217099/Z/19/Z). Research reported in this publication was supported by an institutional startup fund from Texas A&M University (AAZ). DSC was supported by the European Molecular Biology Organization (EMBO) with a long-term EMBO fellowship (ALTF 62-2021). The work benefited from the Imaging Facility, Department of Zoology, supported by Matt Wayland and Tom Pettini, and funds from a Wellcome Trust Equipment Grant (WT079204) with contributions by the Sir Isaac Newton Trust in Cambridge, including Research Grant [18.07ii(c)]. Work on this project further benefited from the Manchester Fly Facility, established through funds from the University and the Wellcome Trust (grant 087742/Z/08/Z).

The authors would like to thank members of the Baines and Landgraf research teams for feedback on the manuscript. The authors are grateful to Ela Serpe for Rabbit polyclonal anti-GluRIIB antiserum.

Stocks obtained from the Bloomington Drosophila Stock Center (NIH P40OD018537) were used in this study.

The 8B4D2 (MH2B) monoclonal antibody to visualise GluRIIA, developed C. Goodman, was obtained from the Developmental Studies Hybridoma Bank, created by the NICHD of the NIH and maintained at The University of Iowa, Department of Biology, Iowa City, IA 52242.

Materials and Methods

Fly husbandry

Wild-type and transgenic strains were maintained on standard yeast–agar–cornmeal medium at 25˚C. For CP manipulations, animals were kept in laying pots with apple juice agar plates and yeast paste for 6h. Collected eggs were either kept at 25°C for controls or at 32°C for 24h, before being moved back to 25°C until animals developed to wandering L3 larvae.

Dissection and Immunostainings

Wandering L3 larvae were dissected in Sørensen's sodium phosphate buffered saline (0.1 M, pH 7.2) and fixed for 10min at room temperature with Bouin´s fixative (Sigma-Aldrich). After fixing, specimens were washed in washing solution (Sørensen's buffer + 0,25% BSA + 0,3% TritonX-100 from Sigma-Aldrich) and incubated with mouse nc82 (anti-Bruchpilot to reveal active zones) antibody (1:100, DSHB) overnight, visualized with goat α-mouse StarRed (1:1000, Abberior, cat.no.STRED-1001-500UG, Lot. 2042PK-1) and AlexaFluor488 conjugated goat α-HRP (1:1000, Jackson ImmunoResearch, cat.no. 123-545-021, Lot. 152767) to visualise presynaptic, neuronal structures. For stainings of the postsynaptic glutamate receptor subunits GluRIIA and GluRIIB we used monoclonal mouse-α-DGluRIIA antibody (1:100, DSHB, product ID: 8B4D2 (MH2B)) and polyclonal rabbit-α-DGluRIIB antiserum (1:1000, gift from Mihaela Serpe (Sulkowski et al., 2016)) in conjunction with goat α-mouse StarRed (1:1000) and goat α-rabbit Atto594 secondary antibodies (1:1000, Hypermol, cat.no. 2306, Lot. 0356RG22), respectively, in combinations with AlexaFluor488 conjugated goat α-HRP (1:1000, Jackson ImmunoResearch, cat.no. 123-545-021, Lot. 152767) to visualise presynaptic terminals.

Fly stocks

Genotype	Phenotype	FlyBase identifiers
Oregon-R	wildtype control	FBst0002376
Canton S	wildtype control	FBst0064349
w^{1118}; ; GMR94G06-GAL4 [attP2]	Targets GAL4 expression selectively to the aCC motoneuron during embryonic and larval stages; kindly gifted by Juan J. Pérez Moreno (Pérez-Moreno and O'Kane, 2019).	FBti0139793
w^{1118}; ; 20XUAS-IVS-jGCaMP8f [VK00005]	GCaMP calcium imaging	FBti0215881
w^{1118}; ; P{y[+t7.7] w[+mC]=GMR36G02-GAL4}attP2	Expresses GAL4 in A27h and M neurons, plus two ventral cells per hemi-neuromere, used for calcium imaging.	FBti0135233
w^{1118}; 34F03 AD [attP40] ; 36G02-DBD [attP2]	A27h neuron driver used for whole cell patching A27h.	
w^{1118}; 20XUAS-Chronos-mVenus [attP40]	Red-shifted channel rhodopsin line used to excite the A27h premotor interneuron to measure its synaptic drive to the aCC motoneuron.	FBti0195682

Image acquisition

Confocal images were acquired, using a Leica Stellaris point scanning confocal microscope, with an 40x/1.25N.A. oil immersion lens (Leica) and a 1.25 digital zoom. Images were acquired with a voxel size 0.16x 0.16x 0.3 µm. Images were processed using FIJI and Affinity Designer.

Two electrode voltage clamp

Two Electrode Voltage Clamp (TEVC) recordings were performed in HL3.1 saline (Feng et al., 2004) composition in mM: NaCl 70, KCl 2.5, $MGCl_2$ 4, $CaCl_2$ 2 (if not other mentioned), $NaHCO_3$ 10, trehalose 5, sucrose 115, HEPES 5 (pH was adjusted to 7.24-7.25 with 1M NaOH), using an Olympus BX50WI compound microscope with 60X dipping (Olympus 60x/0.9 N.A.) objective lenses. Experiments were performed on third-instar larval NMJs of the dorsal acute muscle 1 (DA1) in segments A3 and A4. The respective nerve was sucked in with a self-built suction electrode (Johnson et al., 2007) which was filled with HL3.1 saline. Subsequently, the nerve was stimulated for 0.1ms to trigger action potential firing. Briefly,

voltage was stepwise increased until the first synaptic transmission could be recorded. From that voltage, 1 V was added to reliably evoke APs in control conditions, in 32°C CP manipulated animals 2-3 V had to be added to reliably recruit aCC and RP2. For PhTx experiments, samples were incubated in 4 µM PhTx final concentration (Frank et al., 2006) for 10 min. While dissecting, great care was taken to not stretch animals too much. Successful PhTx application was determined by dividing miniature EPSC amplitude of PhTx treated animals by the average Amplitude of control mEPSCs. If PhTx treated mEPSCs were at least 40% reduced compared to control, PhTx application was considered successful (Frank et al., 2006). Quantal content was determined by dividing EPSC by mEPSC for each recording. Recordings were only further considered from cells with an initial Vm below -50 mV and input resistance between 8-10 MΩ, using intracellular electrodes filled with 3M KCl with resistances of ~20 MΩ (Electrodes for current injection and the membrane voltage). Current passing und recording electrodes were pulled from Borosilicate glass microelectrodes with filament (OD1 mm, ID 0.58mm; Harvard Apparatus LTD, GC100F-10 Part No. 30-0019), suction electrodes from Borosilicate glass microelectrodes without filament (OD1 mm, ID 0.58mm; Harvard Apparatus LTD, GC100-10 Part No. 30-0016) with a Flaming/Brown Puller Model P-97 (Sutter Instruments USA). Excitatory postsynaptic currents (EPSCs) were evoked by an Isolated Pulse Stimulator (Model 2100 A-M Systems USA), recorded at a clamped voltage of -60 mV with a sampling rate of 50 kHz and filtered with the anti-alias filter at 25 kHz using the AxoClamp 2B amplifier (Molecular Devices Axon Instruments USA). Data analysis was done with Clampfit 10.7. Traces were first filtered with a 360 Hz Gaussian low pass filter, then template searches were run over the trace for single pulses and spontaneous miniature excitatory postsynaptic currents (mEPSCs or minis). The resulting files were used to analyse mEPSC and EPSC properties. Rise and decay tau were measured with an one-term exponential product fit (Levenberg-Marquadt method with a max of 5000 iterations)

Current clamp muscle recordings

Current clamp recordings from muscle DA1 were performed in HL3.1 saline (see above), in semi intact, fillet dissected wandering L3 larvae with intact nervous system. After finishing the dissection, only animals performing crawling-like movements were considered for further experiments. To block muscle contractions, a 500 µM stock solution of nifedipine in HL3.1 and 1% DMSO was added to the bath for a final concentration of 50 µM nifedipine and 0.1% DMSO for 15 min. Recordings were only further considered from cells with an initial Vm

below -60 mV and input resistance between 8-10 MΩ, using intracellular electrodes filled with 3M KCl with resistances of ~20 MΩ. Spontaneous activity was recorded for 5min. Burst analysis was performed using the Clampfit Burst Analysis, using the Poisson Surprise model with a minimum of 5 events per burst.

Electroshock assay

A handheld stimulator consisting of two tungsten wires (0.1 mm diameter) fixed to a plastic rod was used. Wires were shaped to be ~1-2 mm apart, attached to a DS2A Mk.II stimulator (Digitimer Ltd), which was set to provide a 6 V, 2 s current pulse. Larvae were placed on a plastic plate lid, with tissue paper used to dry residual moisture from the larvae. Once larvae had returned to normal crawling, the tungsten wires were brought into contact with the larvae, positioned on the larval cuticle, perpendicular to and over the approximate position of the CNS, with gentle pressure. Current stimulation was then delivered, which usually induced a sustained contraction and paralysis representing a seizure (videos can be viewed in Marley and Baines 2011). The time to resumption of normal behaviour (regular, whole body forward propagating peristaltic waves) was recorded and defined as the duration of recovery from seizure.

Dissection and CNS mounting for calcium imaging and electrophysiology

Larval CNSs were dissected and mounted for electrophysiological recordings and for GCaMP imaging. Third instar (L3) larvae (of either sex) were dissected in a dish in standard saline (135 mM NaCl (Fisher Scientific), 5 mM KCl (Fisher Scientific), 4 mM $MgCl_2 \cdot 6H_2O$ (Sigma-Aldrich), 2mM $CaCl_2 \cdot 2H_2O$ (Fisher Scientific), 5 mM TES (Sigma-Aldrich), 36 mM sucrose (Fisher Scientific), pH 7.15), to remove the CNS (ventral nerve cord and brain lobes). The isolated CNS was then transferred to a droplet of external saline, within which it was laid flat (dorsal side up) and glued (GLUture Topical Tissue Adhesive; World Precision Instruments USA) to a Sylgard-coated cover slip (1 to 2mm depth of cured SYLGARD Elastomer (Dow-Corning USA) on a 22 x 22mm square coverslip). The preparation was then placed on a glass slide and viewed under a microscope (Olympus BX51-WI).

Calcium imaging

Dissected CNSs were imaged (QImaging EXi-Aqua; photometrics, Arizona, US) with an acquisition frame rate of 10Hz and frame duration of 100 ms using a x20 immersion lens. GCaMP8f was excited using a 470 nm collimated LED (Thorlabs, New Jersey, US). Time-course of neuronal fluorescence was determined in WinFluor (V.4.1.5; University of Strathclyde, UK) by adding regions of interest (ROIs) to axons, close to the cell body (Streit et al, 2016). In Clampfit (10.3.1.5; Molecular Devices, California, US) fluorescence traces were smoothed using a lowpass BoxCar filter using 11 smoothing points prior to analysis.

For motoneuron calcium transients (Fig.1), recordings were conducted for 600s, whilst temperature of the explanted CNS was increased steadily from ~23°C to ~34°C using a digital heating unit (CO 102; Linkam Scientific, Surrey, UK). For sham recordings, temperature was maintained at a constant 25°C. Temperature was measured in Clampex (10.3.1.5; Molecular Devices, California, US) using a temperature sensor placed in the external saline surrounding the brain, via a temperature controller (TC-10; npi electronic GmbH, Tamm, Germany). The frequency of calcium fluorescence peaks was measured for each segment (A8/9 – A1) in three sequential 200 s time periods and averaged per larva. Average temperature was calculated for each recording during these same 200 s time periods.

For calcium imaging of interneurons after CP manipulation (Fig.5), 180 s recordings were taken. Time lag was determined by manually assessing the time between peak fluorescence corresponding to ipsilaterally adjacent interneurons (segments A6 – A1. For each recording the first complete forward waves of activity were used (up to three repeats per trace) to generate an average intersegment duration for each pair of interneurons.

Whole cell patch clamp electrophysiology

CNSs were dissected, mounted (see calcium imaging methods) and viewed under a 60x water-immersion lens. To access soma, 1% protease (Streptomyces griseus, Type XIV, Sigma-Aldrich, in external saline) contained within a wide-bore glass pipette (GC100TF-10; Harvard Apparatus UK, approx. 10 µm opening) was applied to abdominal segments, roughly between A5-A2 (Baines and Bate, 1998). This was done to remove overlaying glia to facilitate access to underlying nerve cell soma (e.g., aCC). Motoneurons were identified by anatomical position and relative cell size, with aCC being positioned close to the midline and containing both an ipsilateral and contralateral projection. Recordings were made using

borosilicate glass pipettes (GC100F-10, Harvard Apparatus) that were fire polished to resistances of 10 - 15MΩ when filled with intracellular saline (140 mM potassium-D-gluconate (Sigma-Aldrich), 2 mM $MgCl_2 \cdot 6H_2O$ (Sigma-Aldrich), 2 mM EGTA (Sigma-Aldrich), 5 mM KCl (Fisher Scientific), and 20 mM HEPES (Sigma-Aldrich), (pH 7.4). Input resistance was measured in the 'whole cell' configuration, and only cells that had an input resistance ≥ 0.5 GΩ were used for experiments. Cell capacitance and break-in resting membrane potential was also measured for each cell recorded. Data for current steps recordings was captured using a Multiclamp 700B amplifier controlled by pCLAMP (version 10.7.0.3), via an analogue-to-digital converter (Digidata 1440A, Molecular Devices). Whole cell recordings measuring synaptic drive to motoneurons and spontaneous motoneurons activity were conducted using an amplifier (Axopatch 1D) controlled by pCLAMP (V.10.3.1.5) by an analog-to- digital converter (Digidata 1322A, Molecular Devices. Trace/s were sampled at 20 kHz and filtered online at 10 kHz.

Current step recordings

Mecamylamine (200 μM in saline) was used to block postsynaptic nACh receptors in order to synaptically isolate neurons for experiments designed to measure intrinsic motoneuron excitability. Once patched, neurons were brought to a membrane potential of -60 mV using current injection. Each recording consisted of 20 x 4 pA (500 ms) current steps, including an initial negative step, giving a range of -4 to +72 pA. Number of spikes were counted and plotted against injected current. Both cell capacitance and input resistance were compared between conditions to ensure that any observed differences in excitability were not due to differences in either cell size or resistance.

Synaptic drive to motoneurons

To measure synaptic drive between A27h premotor interneurons and aCC, A27h neurons were identified via *Chronos-mVenus* reporter (as above), allowing corresponding aCC motoneurons to be patched. Recordings were conducted in current-clamp, with current injected into aCC sufficient to evoke a mean spike frequency of ~10-20 Hz, prior to optogenetic stimulation. Recordings consisted of: individual sweeps, beginning with 1 s LED off, followed by 1 s LED on, and 1 s LED off (repeated 5-8 times per cell). Change in AP frequency (%) was calculated for each recording (per sweep) comparing AP frequency before and during stimulation, which was then averaged for each cell.

Spontaneous rhythmic currents (SRCs) were recorded for 180 s with aCC voltage clamped at -60 mV. Amplitude, duration, and frequency were measured for the first 15 events of each trace using Clampfit's event detection, threshold search, function. The first 15 events with a stable baseline, an amplitude of >300 pA and no double peaks were accepted for analysis. Amplitude was measured as the change from baseline immediately prior to event initiation to the peak current and normalised for cell capacitance, providing a measure of current density. SRC duration was measured as the width of an event at 100 pA amplitude.

Spontaneous motoneuron recordings

Motoneuron spontaneous activity was recorded using an adapted whole cell current clamp protocol, in I=0, to measure passive action potential bursting properties. In Clampfit (version 10.3.1.5), 180 s recordings, were analysed to detect action potential 'spike times'. These were imported into MATLAB and analysed using a custom script (developed by Mituzaite et al., 2021). An action potential burst was considered as an event consisting of at least 3 spikes occurring within 100 ms and ending when no spike was detected for 100 ms.

Crawling Assay

Crawling behaviour was recorded at the mid-third instar stage, 72 hours after larval hatching (ALH). Larvae were rinsed in water and placed inside a 24cm x 24cm crawling arena with a base of 5mm thick 0.8% agarose gel (Bacto Agar), situated inside an incubator. Temperature was maintained at 25±0.5°C, reported via a temperature probe in the agar medium. Humidity was kept constant. Larval crawling was recorded using a frustrated total internal reflection-based imaging method (FIM) in conjunction with the tracking software FIMTrack (Risse et al., 2017, 2013) using a Basler acA2040-180km CMOS camera, fitted with a 16mm KOWA-IJM3sHC.SW-VIS-NIR lens, acquisition controlled by Pylon software (Basler) and Streampix (v.6) software (NorPix). Larvae were recorded for 20 minutes at five frames per second.

Recordings were split into four 5-minute sections with the first five minutes of acclimatisation discarded. The remaining three 5-minute sections were used to analyse crawling speed, choosing crawling periods of uninterrupted forward crawling, devoid of pauses, turning or collision events. Each larva was sampled up to once per 5-minute section. Crawling speed was calculated using FIMTrack software.

Statistics

Statistical analyses were done using GraphPad Prism Software (Version 10.1.2). Datasets were tested for normal distribution with the Shapiro-Wilk Test. Normally distributed data were then tested with students t-test (for pairwise comparison). Normally distributed analysis for

more than two groups was done with a one-way ANOVA and post hoc tested with a Tukey multiple comparison test. Non-normally distributed data sets of two groups were tested with Mann-Whitney U Test (pairwise comparison) and datasets with more than two groups were tested with a Kruskal Wallis ANOVA and post hoc tested with a Dunns multiple post hoc comparison test. For whole cell electrophysiology experiments in isolated neurons, linear regression analysis was used to compare the intercepts between conditions. This analysis was restricted to linear sections of data, represented by inset graphs. For all datasets mean and standard error of mean (SEM) are shown. Significance levels were * $p<0.05$; ** $p<0.01$; *** $p<0.001$; **** $p<0.0001$

References

Ackerman SD, Perez-Catalan NA, Freeman MR, Doe CQ. Astrocytes close a motor circuit critical period. 2021. Nature **592**:414-420. doi:10.1038/s41586-021-03441-2

Ashburner M, Carson HL, Thompson JN. 1983. Ectophysilogy: Abiotic FactorsThe Genetics and Biology of Drosophila,. pp. 105–170.

Baines RA, Robinson SG, Fujioka M, Jaynes JB, Bate M. 1999. Postsynaptic expression of tetanus toxin light chain blocks synaptogenesis in Drosophila. *Current Biology* **9**:1267-S1. doi:10.1016/S0960-9822(99)80510-7

Baines RA, Uhler JP, Thompson A, Sweeney ST, Bate M. 2001. Altered Electrical Properties in Drosophila Neurons Developing without Synaptic Transmission. *The Journal of Neuroscience* **21**:1523–1531. doi:10.1523/JNEUROSCI.21-05-01523.2001

Baumann NS, Sears JC, Broadie K. 2024. Experience-dependent MAPK/ERK signaling in glia regulates critical period remodeling of synaptic glomeruli. *Cell Signal* **120**:111224. doi:10.1016/j.cellsig.2024.111224

Carreira-Rosario A, York RA, Choi M, Doe CQ, Clandinin TR. 2021. Mechanosensory input during circuit formation shapes Drosophila motor behavior through patterned spontaneous network activity. *Current Biology* **31**:5341-5349.e4. doi:10.1016/j.cub.2021.08.022

Chodankar A, Sadanandappa MK, VijayRaghavan K, Ramaswami M. 2020. Glomerulus-Selective Regulation of a Critical Period for Interneuron Plasticity in the *Drosophila* Antennal Lobe. *The Journal of Neuroscience* **40**:5549–5560. doi:10.1523/JNEUROSCI.2192-19.2020

Corke J, Huertas Radi M, Landgraf M, Baines RA. 2025. Maturation of GABAergic signalling times the opening of a critical period in *Drosophila melanogaster*. doi:10.1101/2025.04.24.650400

Coulson B, Hunter I, Doran S, Parkin J, Landgraf M, Baines RA. 2022. Critical periods in Drosophila neural network development: Importance to network tuning and therapeutic potential. *Front Physiol* **13**:1–11. doi:10.3389/fphys.2022.1073307

Crisp S, Evers JF, Fiala A, Bate M. 2008. The development of motor coordination in Drosophila embryos. *Development* **135**:3707–3717. doi:10.1242/dev.026773

Crisp SJ, Evers JF, Bate M. 2011. Endogenous Patterns of Activity Are Required for the Maturation of a Motor Network. *Journal of Neuroscience* **31**:10445–10450. doi:10.1523/JNEUROSCI.0346-11.2011

Delvendahl I, Müller M. 2019. Homeostatic plasticity—a presynaptic perspective. *Curr Opin Neurobiol* **54**:155–162. doi:10.1016/j.conb.2018.10.003

Dombrovski M, Condron B. 2021. Critical periods shaping the social brain: A perspective from Drosophila. *BioEssays* **43**:2000246. doi:10.1002/bies.202000246

Dyson A, Ryan M, Garg S, Evans DG, Baines RA. 2022. Loss of NF1 in Drosophila Larvae Causes Tactile Hypersensitivity and Impaired Synaptic Transmission at the Neuromuscular Junction. *Journal of Neuroscience* **42**:9450–9472. doi:10.1523/JNEUROSCI.0562-22.2022

Feng Y, Ueda A, Wu CF. 2004. A modified minimal hemolymph-like solution, HL3.1, for physiological recordings at the neuromuscular junctions of normal and mutant Drosophila larvae. *J Neurogenet* **18**:377–402. doi:10.1080/01677060490894522

Frank CA, James TD, Müller M. 2020. Homeostatic control of Drosophila neuromuscular junction function. *Synapse* **74**:22133. doi:10.1002/syn.22133

Frank CA, Kennedy MJ, Goold CP, Marek KW, Davis GW. 2006. Mechanisms Underlying the Rapid Induction and Sustained Expression of Synaptic Homeostasis. *Neuron* **52**:663–677. doi:10.1016/j.neuron.2006.09.029

Fujioka M, Lear BC, Landgraf M, Yusibova GL, Zhou J, Riley KM, Patel NH, Jaynes JB. 2003. Even-skipped, acting as a repressor, regulates axonal projections in Drosophila. *Development* **130**:5385–5400. doi:10.1242/dev.00770

Fushiki A, Kohsaka H, Nose A. 2013. Role of Sensory Experience in Functional Development of Drosophila Motor Circuits. *PLoS One* **8**:e62199. doi:10.1371/journal.pone.0062199

Genç Ö, Davis GW. 2019. Target-wide Induction and Synapse Type-Specific Robustness of Presynaptic Homeostasis. *Current Biology* **29**:3863-3873.e2. doi:10.1016/j.cub.2019.09.036

Giachello CNG, Baines RA. 2015. Inappropriate Neural Activity during a Sensitive Period in Embryogenesis Results in Persistent Seizure-like Behavior. *Current Biology* **25**:2964–2968. doi:10.1016/j.cub.2015.09.040

Giachello CNG, Fan YN, Landgraf M, Baines RA. 2021. Nitric oxide mediates activity-dependent change to synaptic excitation during a critical period in Drosophila. *Sci Rep* **11**:1–12. doi:10.1038/s41598-021-99868-8

Giachello CNG, Fan YN, Landgraf M, Baines RA. 2019. Activity manipulation of an excitatory interneuron, during an embryonic critical period, alters network tuning of the Drosophila larval locomotor circuit. *bioRxiv*. doi:10.1101/780221

Giachello CNG, Zarin AA, Kohsaka H, Fan YN, Nose A, Landgraf M, Baines RA. 2020. Electrophysiological validation of premotor interneurons monosynaptically connected to the aCC motoneuron in the Drosophila larval CNS. *bioRxiv* 1–19. doi:10.1101/2020.06.17.156430

Goel P, Dickman D. 2021. Synaptic homeostats: latent plasticity revealed at the Drosophila neuromuscular junction. *Cellular and Molecular Life Sciences*. doi:10.1007/s00018-020-03732-3

Hageter J, Starkey J, Horstick EJ, Hageter J, Starkey J, Horstick EJ. 2023. Article Thalamic regulation of a visual critical period and motor behavior ll ll Thalamic regulation of a visual critical period and motor behavior. *CellReports* **42**:112287. doi:10.1016/j.celrep.2023.112287

Harrison R V, Gordon KA, Mount RJ. 2005. Is There a Critical Period for Cochlear Implantation in Congenitally Deaf Children ? Analyses of Hearing and Speech Perception Performance after Implantation. *Dev Psychobiol* **46**:155–292. doi:DOI 10.1002/dev.20052

Heckman EL, Doe CQ. 2022. Presynaptic contact and activity opposingly regulate postsynaptic dendrite outgrowth. *Elife* **11**. doi:10.7554/eLife.82093

Hensch TK. 2005. Critical period plasticity in local cortical circuits. *Nat Rev Neurosci*. doi:10.1038/nrn1787

Hensch TK, Quinlan EM. 2018. Critical periods in amblyopia. *Vis Neurosci*. doi:10.1017/S0952523817000219

Hess EH. 1975. Imprinting: Early experience and the dvelopmental psychobiology of attachment. *Psychosom Med* **37**:188–190.

Horn G. 2004. Pathways of the past: the imprint of memory. *Nat Rev Neurosci* **5**:108–121. doi:10.1038/nrn1324

Hubel DH, Wiesel TN. 1970. The period of susceptibility to the physiological effect of unilateral eye closure in kittens. *Journal of Physiology* **206**:419–436. doi:10.1113/jphysiol.1970.sp009022

Hunter I, Coulson B, Pettini T, Davies JJ, Parkin J, Landgraf M, Baines RA. 2024. Balance of activity during a critical period tunes a developing network. *Elife* **12**:1–23. doi:10.7554/eLife.91599

Hunter I, Coulson B, Zarin AA, Baines RA. 2021. The Drosophila Larval Locomotor Circuit Provides a Model to Understand Neural Circuit Development and Function. *Front Neural Circuits*. doi:10.3389/fncir.2021.684969

Johnson BR, Hauptman SA, Bonow RH. 2007. Construction of a Simple Suction Electrode for Extracellular Recording and Stimulation. *Journal of Undergraduate Neuroscience Education* **6**:A21.

Jusyte M, Blaum N, Böhme MA, Berns MMM, Bonard AE, Vámosi ÁB, Pushpalatha K V., Kobbersmed JRL, Walter AM. 2023. Unc13A dynamically stabilizes vesicle priming at synaptic release sites for short-term facilitation and homeostatic potentiation. *Cell Rep* **42**. doi:10.1016/j.celrep.2023.112541

Kiral FR, Dutta SB, Linneweber GA, Hilgert S, Poppa C, Duch C, von Kleist M, Hassan BA, Hiesinger PR. 2021. Brain connectivity inversely scales with developmental temperature in Drosophila. *Cell Rep* **37**:110145. doi:10.1016/j.celrep.2021.110145

Kratschmer P, Lowe SA, Buhl E, Chen K, Kullmann DM, Pittman A, Hodge JJL, Jepson JEC. 2021. Impaired Pre-Motor Circuit Activity and Movement in a Drosophila Model of KCNMA1 -Linked Dyskinesia. *Movement Disorders* **36**:1158–1169. doi:10.1002/mds.28479

Landgraf M, Jeffrey V, Fujioka M, Jaynes JB, Bate M. 2003. Embryonic Origins of a Motor System: Motor Dendrites Form a Myotopic Map in Drosophila. *PLoS Biol* **1**:e41. doi:10.1371/journal.pbio.0000041

Lee Y, Montell C. 2013. Drosophila TRPA1 functions in temperature control of circadian rhythm in pacemaker neurons. *Journal of Neuroscience* **33**:6716–6725. doi:10.1523/JNEUROSCI.4237-12.2013

Leier HC, Foden AJ, Jindal DA, Wilkov AJ, Van der Linden Costello P, Vanderzalm PJ, Coutinho-Budd J, Tabuchi M, Broihier HT. 2025. Glia control experience-dependent plasticity in an olfactory critical period. *Elife* **13**. doi:10.7554/eLife.100989

Lowe SA, Wilson AD, Aughey GN, Banjaree A, Goble T, Simon-Batsford N, Sanderson A, Kratschmer P, Balogun M, Gao H, Aw SS, Jepson JEC. 2023. BK channel gain-of-function disrupts limp control by suppressing neurotransmission during a critical developmental window. *bioRxiv*. doi:10.1101/2023.09.20.558625

Marder E. 2023. Individual Variability, Statistics, and the Resilience of Nervous Systems of Crabs and Humans to Temperature and Other Perturbations. *eNeuro* **10**:ENEURO.0425-23.2023. doi:10.1523/ENEURO.0425-23.2023

Marder E, Rue MCP. 2021. From the Neuroscience of Individual Variability to Climate Change. *The Journal of Neuroscience* **41**:10213–10221. doi:10.1523/JNEUROSCI.1261-21.2021

Mòdol L, Moissidis M, Selten M, Oozeer F, Marín O. 2024. Somatostatin interneurons control the timing of developmental desynchronization in cortical networks. Neuron **112**:2015-2030.e5. doi: 10.1016/j.neuron.2024.03.014

Müller M, Davis GW. 2012. Transsynaptic control of presynaptic Ca 2+ influx achieves homeostatic potentiation of neurotransmitter release. *Current Biology* **22**:1102–1108. doi:10.1016/j.cub.2012.04.018

Nardou R, Sawyer E, Song YJ, Wilkinson M, Padovan-Hernandez Y, de Deus JL, Wright N, Lama C, Faltin S, Goff LA, Stein-O'Brien GL, Dölen G. 2023. Psychedelics reopen the social reward learning critical period. *Nature* **618**:790–798. doi:10.1038/s41586-023-06204-3

Nelson N, Vita DJ, Broadie K. 2024. Experience-dependent glial pruning of synaptic glomeruli during the critical period. *Sci Rep* **14**:9110. doi:10.1038/s41598-024-59942-3

Oswald MCW, Brooks PS, Zwart MF, Mukherjee A, West RJH, Giachello CNG, Morarach K, Baines RA, Sweeney ST, Landgraf M. 2018. Reactive oxygen species regulate activity-dependent neuronal plasticity in Drosophila. *Elife* **7**. doi:10.7554/eLife.39393

Peled ES, Isacoff EY. 2011. Optical quantal analysis of synaptic transmission in wild-type and rab3-mutant Drosophila motor axons. *Nat Neurosci* **14**:519–526. doi:10.1038/nn.2767

Pérez-Moreno JJ, O'Kane CJ. 2019. GAL4 Drivers Specific for Type Ib and Type Is Motor Neurons in Drosophila. *G3 Genes|Genomes|Genetics* **9**:453–462. doi:10.1534/g3.118.200809

Powsner L. 1935. The Effects of Temperature on the Durations of the Developmental Stages of Drosophila melanogaster. *Physiol Zool* **8**:474–520. doi:10.1086/physzool.8.4.30151263

Pulver SR, Bayley TG, Taylor AL, Berni J, Bate M, Hedwig B. Imaging fictive locomotor patterns in larval Drosophila. 2015. J Neurophysiol **114**:2564-77. doi: 10.1152/jn.00731.2015

Reh RK, Dias BG, Nelson CA 3rd, Kaufer D, Werker JF, Kolb B, Levine JD, Hensch TK. 2020. Critical period regulation across multiple timescales. Proc Natl Acad Sci U S A **117**:23242-23251. doi: 10.1073/pnas.1820836117

Risse B, Berh D, Otto N, Klämbt C, Jiang X. 2017. FIMTrack: An open source tracking and locomotion analysis software for small animals. *PLoS Comput Biol* **13**:1–15. doi:10.1371/journal.pcbi.1005530

Risse B, Thomas S, Otto N, Löpmeier T, Valkov D, Jiang X, Klämbt C. 2013. FIM, a Novel FTIR-Based Imaging Method for High Throughput Locomotion Analysis. *PLoS One* **8**:1–11. doi:10.1371/journal.pone.0053963

Scialò F, Sriram A, Naudí A, Ayala V, Jové M, Pamplona R, Sanz A. 2015. Target of rapamycin activation predicts lifespan in fruit flies. *Cell Cycle* **14**:2949–2958. doi:10.1080/15384101.2015.1071745

Sigrist SJ, Reiff DF, Thiel PR, Steinert JR, Schuster CM. 2003. Experience-Dependent Strengthening of Drosophila Neuromuscular Junctions. *The Journal of Neuroscience* **23**:6546–6556. doi:10.1523/JNEUROSCI.23-16-06546.2003

Soiza-Reilly M, Azcurra JM. 2009. Developmental striatal critical period of activity-dependent plasticity is also a window of susceptibility for haloperidol induced adult motor alterations. *Neurotoxicol Teratol* **31**:191–197. doi:10.1016/j.ntt.2009.03.001

Streit AK, Fan YN, Masullo L, Baines RA. 2016. Calcium Imaging of Neuronal Activity in Drosophila Can Identify Anticonvulsive Compounds. PLoS One **11**:e0148461. doi: 10.1371/journal.pone.0148461

Sulkowski MJ, Han TH, Ott C, Wang Q, Verheyen EM, Lippincott-Schwartz J, Serpe M. 2016. A Novel, Noncanonical BMP Pathway Modulates Synapse Maturation at the Drosophila Neuromuscular Junction. *PLoS Genet* **12**:e1005810. doi:10.1371/journal.pgen.1005810

Valdes-Aleman J, Fetter RD, Sales EC, Heckman EL, Venkatasubramanian L, Doe CQ, Landgraf M, Cardona A, Zlatic M. 2021. Comparative Connectomics Reveals How Partner Identity, Location, and Activity Specify Synaptic Connectivity in Drosophila. *Neuron* **109**:105-122.e7. doi:10.1016/j.neuron.2020.10.004

Williamson M, Mitchell A, Condron B. 2021. Birth temperature followed by a visual critical period determines cooperative group membership. *J Comp Physiol A Neuroethol Sens Neural Behav Physiol* **207**:739–746. doi:10.1007/s00359-021-01512-3

Winding M, Pedigo BD, Barnes CL, Patsolic HG, Park Y, Kazimiers T, Fushiki A, Andrade I V, Khandelwal A, Valdes-aleman J, Li F, Randel N, Barsotti E, Correia A, Fetter RD, Hartenstein V, Priebe CE, Vogelstein JT, Cardona A, Zlatic M. 2023. The connectome of an insect brain. *Science (1979)* **379**. doi:10.1126/science.add9330

Zeng X, Komanome Y, Kawasaki T, Inada K, Jonaitis J, Pulver SR, Kazama H, Nose A. 2021. An electrically coupled pioneer circuit enables motor development via proprioceptive feedback in Drosophila embryos. *Current Biology* **31**:5327-5340.e5. doi:10.1016/j.cub.2021.10.005

Zhong Y, Wu C-F. 2004. Neuronal Activity and Adenylyl Cyclase in Environment-Dependent Plasticity of Axonal Outgrowth in Drosophila. *The Journal of Neuroscience* **24**:1439–1445. doi:10.1523/JNEUROSCI.0740-02.2004

Züfle P, Batista LL, Brandão SC, D'Uva G, Daniel C, Martelli C. 2025. Impact of developmental temperature on neural growth, connectivity, and function. *Sci Adv* **11**. doi:10.1126/sciadv.adp9587